

## Supporting Information

### Computational Screening of Single Transition–metal Atoms Anchored to g–C<sub>9</sub>N<sub>4</sub> as Catalysts for N<sub>2</sub> Reduction to NH<sub>3</sub>

Xuxin Kang<sup>a</sup>, Junchao Huang<sup>a</sup> and Xiangmei Duan<sup>a,b,\*</sup>

<sup>a</sup> School of Physical Science and Technology, Ningbo University, Ningbo 315211 P. R. China

<sup>b</sup> Laboratory of Clean Energy Storage and Conversion, Ningbo University, Ningbo, P.R.  
China

**Table S1** The adsorption energy ( $E_{*N_2}^{\text{ads}}$ , in eV), the change of Gibbs free energy ( $\Delta G_{*N_2}$ , in eV), and the bond length of N–N ( $d_{\text{N–N}}$ , Å) of  $\text{N}_2$  adsorbed on TM@g-C<sub>9</sub>N<sub>4</sub> in end-on and side-on modes.

TM atom	End-on			Side-on		
	$E_{*N_2}^{\text{ads}}$	$\Delta G_{*N_2}$	$d_{\text{N–N}}$	$E_{*N_2}^{\text{ads}}$	$\Delta G_{*N_2}$	$d_{\text{N–N}}$
Sc	-0.90	-0.46	1.13	-0.53	-0.13	1.15
<b>Ti</b>	-1.09	-0.48	1.14	<b>-0.57</b>	<b>0.09</b>	<b>1.18</b>
V	-0.93	-0.49	1.13	-0.34	0.07	1.15
Cr	-0.42	0.02	1.12	/	/	/
Mn	-0.47	-0.06	1.12	/	/	/
Fe	-0.90	-0.45	1.13	-0.36	0.05	1.15
Co	-0.93	-0.48	1.13	/	/	/
Ni	-0.54	-0.08	1.13	/	/	/
Cu	-0.92	-0.44	1.12	-0.42	0.04	1.14
Zn	-0.46	-0.02	1.12	/	/	/
Y	-0.80	-0.34	1.13	-0.44	-0.03	1.14
<b>Zr</b>	-1.15	-0.72	1.14	<b>-0.70</b>	<b>-0.27</b>	<b>1.18</b>
<b>Nb</b>	-1.24	-0.76	1.15	<b>-0.62</b>	<b>-0.16</b>	<b>1.19</b>
<b>Mo</b>	-0.83	-0.35	1.14	<b>-0.33</b>	<b>0.14</b>	<b>1.19</b>
Ru	-1.11	-0.64	1.14	/	/	/
Rh	-0.65	-0.14	1.13	/	/	/
Pd	-0.38	0.08	1.12	/	/	/
Ag	-0.15	0.19	1.12	/	/	/
Cd	-0.22	0.16	1.11	/	/	/
<b>Hf</b>	-1.13	-0.67	1.14	<b>-0.70</b>	<b>-0.27</b>	<b>1.20</b>
<b>Ta</b>	-1.31	-0.83	1.15	<b>-0.83</b>	<b>-0.36</b>	<b>1.21</b>
<b>W</b>	-1.17	-0.70	1.15	<b>-0.78</b>	<b>-0.29</b>	<b>1.21</b>
<b>Re</b>	-1.44	-0.94	1.15	<b>-0.89</b>	<b>-0.39</b>	<b>1.23</b>
<b>Os</b>	-1.21	-0.72	1.14	<b>-0.41</b>	<b>0.08</b>	<b>1.19</b>
Ir	-0.91	-0.39	1.13	/	/	/
Pt	-0.38	0.09	1.13	/	/	/
Au	-0.11	0.25	1.11	/	/	/

**Table S2** Zero-point energy (ZPE) and entropy (TS, T = 298.15 K) for all reaction intermediates of Nb, W, Re@g-C<sub>9</sub>N<sub>4</sub> via the enzymatic pathway and Ta@g-C<sub>9</sub>N<sub>4</sub> via the distal pathway. \* represent the catalyst.

<b>Nb@g-C<sub>9</sub>N<sub>4</sub></b>	ZPE (eV)	TS (eV)
*N-*N	0.18	0.15
*N-*NH	0.47	0.13
*NH-*NH	0.79	0.14
*NH-*NH <sub>2</sub>	1.13	0.15
*NH <sub>2</sub> -*NH <sub>2</sub>	1.36	0.17
*NH <sub>2</sub>	0.66	0.12
*NH <sub>3</sub>	1.02	0.11

<b>W@g-C<sub>9</sub>N<sub>4</sub></b>	ZPE (eV)	TS (eV)
*N-*N	0.19	0.12
*N-*NH	0.48	0.12
*NH-*NH	0.8	0.14
*NH-*NH <sub>2</sub>	1.13	0.12
*NH <sub>2</sub> -*NH <sub>2</sub>	1.35	0.16
*NH <sub>2</sub>	0.65	0.13
*NH <sub>3</sub>	1.01	0.09

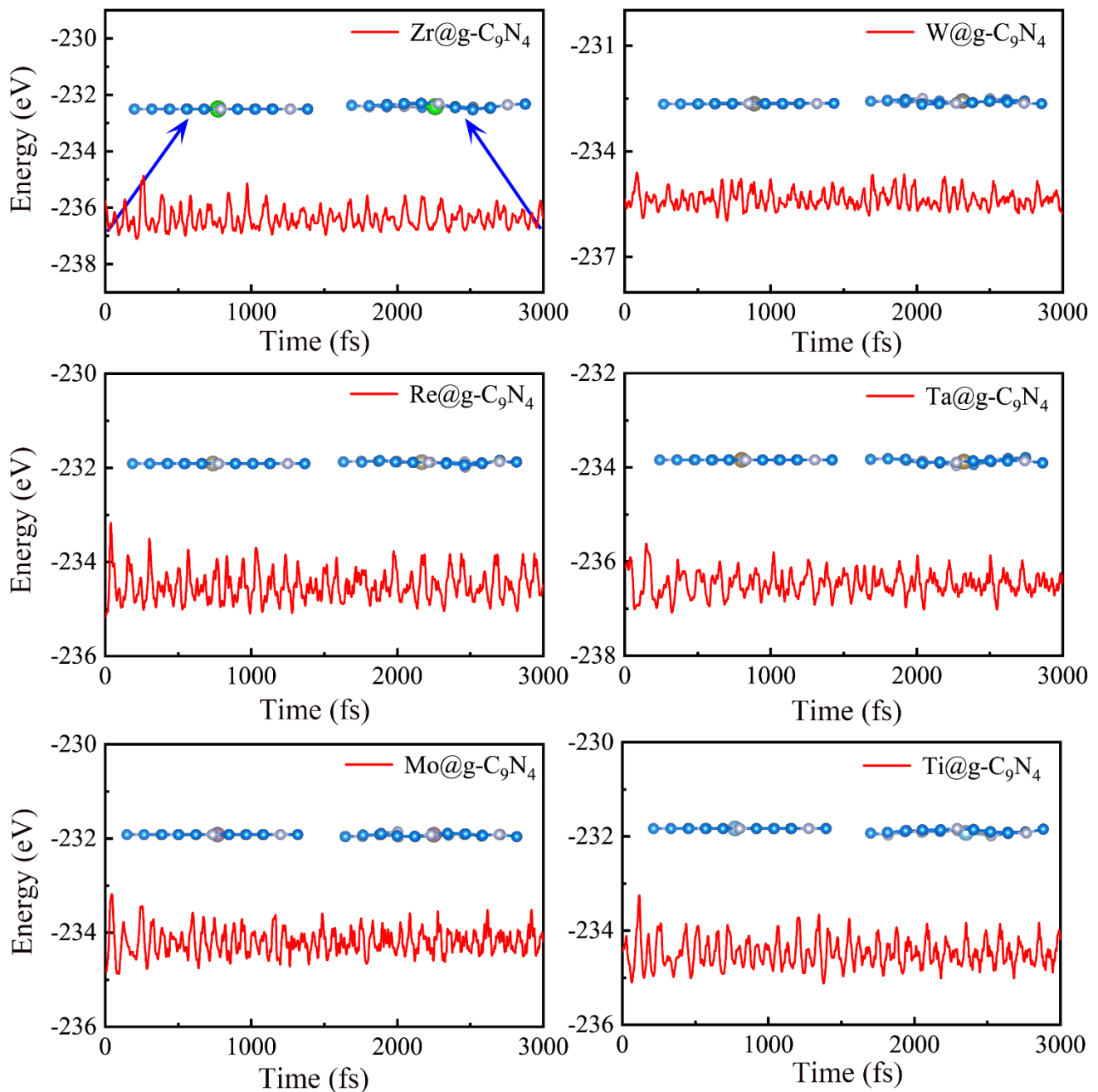
<b>Re@g-C<sub>9</sub>N<sub>4</sub></b>	ZPE (eV)	TS (eV)
*N-*N	0.2	0.11
*N-*NH	0.49	0.11
*NH-*NH	0.82	0.12
*NH-*NH <sub>2</sub>	1.13	0.13
*NH <sub>2</sub> -*NH <sub>2</sub>	1.43	0.11
*NH <sub>2</sub>	0.66	0.11
*NH <sub>3</sub>	1.03	0.08

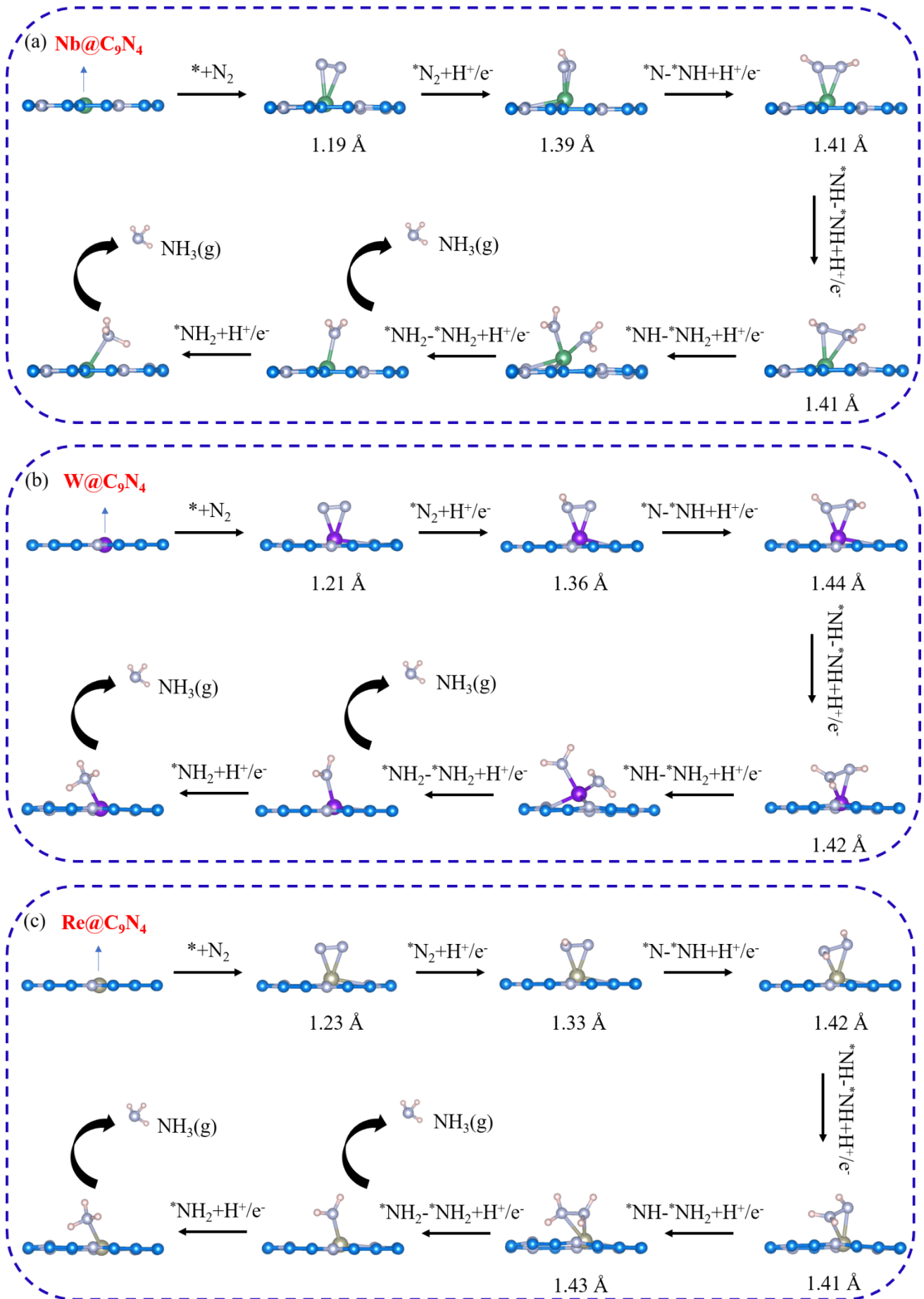
<b>Ta@g-C<sub>9</sub>N<sub>4</sub></b>	ZPE (eV)	TS (eV)
*N-N	0.2	0.15
*N-NH	0.47	0.16
*N-NH <sub>2</sub>	0.81	0.20
*N	0.09	0.05
*NH	0.36	0.08
*NH <sub>2</sub>	0.66	0.12
*NH <sub>3</sub>	1.01	0.10

**Table S3** The adsorption energy ( $E_{\text{H}}$ , in eV) of H on TM, C and N sites of SACs

	$E_{\text{H}}$ (TM site)	$E_{\text{H}}$ (C site)	$E_{\text{H}}$ (N site)
Zr@g-C <sub>9</sub> N <sub>4</sub>	<b>-0.70</b>	0.48	-0.20
Nb@g-C <sub>9</sub> N <sub>4</sub>	<b>-0.64</b>	0.46	-0.28
Ta@g-C <sub>9</sub> N <sub>4</sub>	<b>-0.90</b>	0.54	-0.24
W@g-C <sub>9</sub> N <sub>4</sub>	<b>-0.86</b>	0.77	-0.59
Re@g-C <sub>9</sub> N <sub>4</sub>	<b>-0.96</b>	0.91	-0.66
Ti@g-C <sub>9</sub> N <sub>4</sub>	<b>-0.27</b>	0.69	-0.17
Mo@g-C <sub>9</sub> N <sub>4</sub>	<b>-0.42</b>	0.71	-0.37



**Fig. S1** The variation of energy after AIMD simulation for Zr, W, Re, Ta, Mo and Ti@g-C<sub>9</sub>N<sub>4</sub>. The insets display the initial and final structures of the catalysts at 500 K.



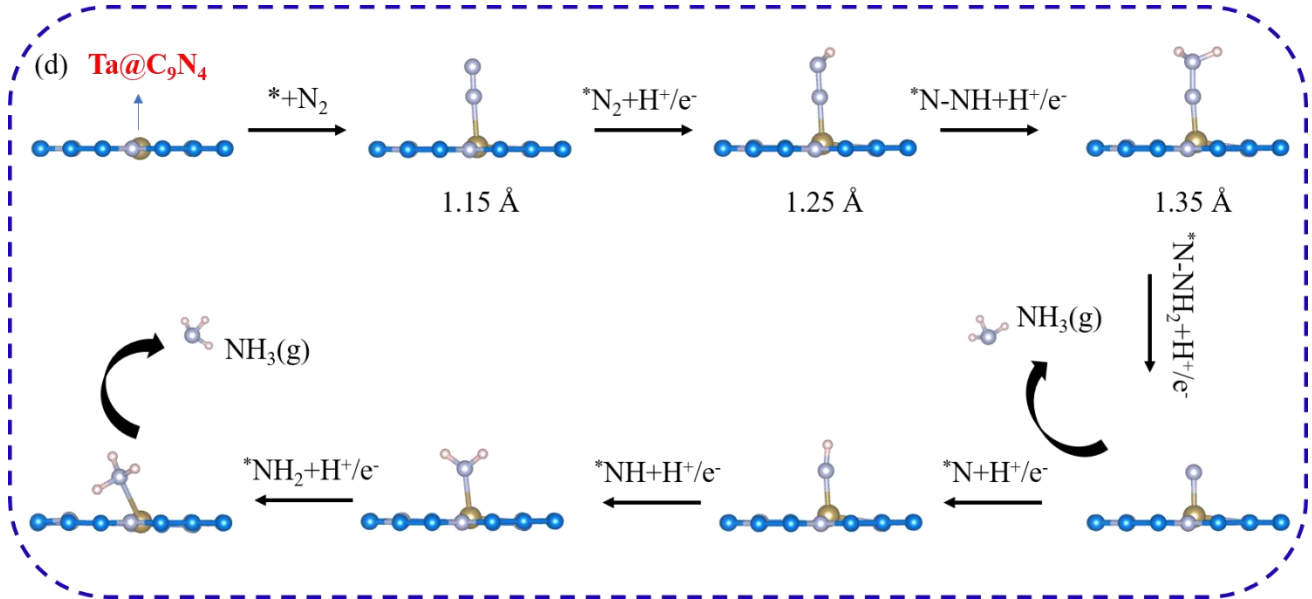


**Fig. S2** Optimized structures of various reduction intermediates on (a) Nb@g-C<sub>9</sub>N<sub>4</sub>, (b) W@g-C<sub>9</sub>N<sub>4</sub>, (c) Re@g-C<sub>9</sub>N<sub>4</sub> through the enzymatic pathway and (d) Ta@g-C<sub>9</sub>N<sub>4</sub> through the distal pathway. N–N bond lengths are presented.

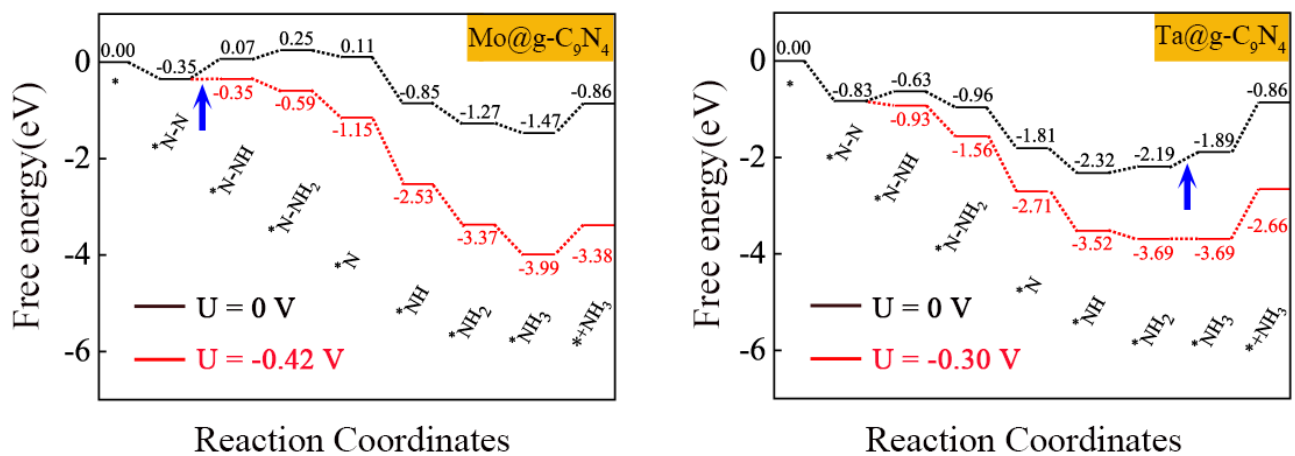


**Fig. S3** Gibbs free energy diagrams of the NRR on Mo@g-C<sub>9</sub>N<sub>4</sub> and Ta@g-C<sub>9</sub>N<sub>4</sub> along distal pathway.

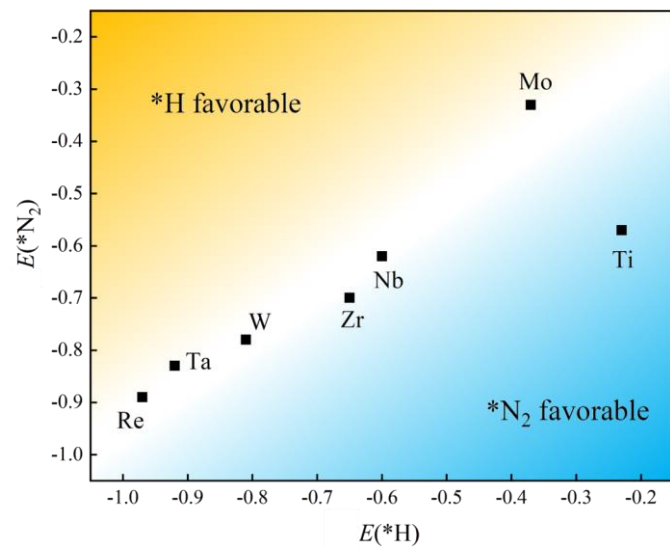


**Fig. S4** The adsorption energy of  $*\text{N}_2$  ( $E(*\text{N}_2)$ ) as a function of adsorption energy H atom ( $E(*\text{H})$ ).

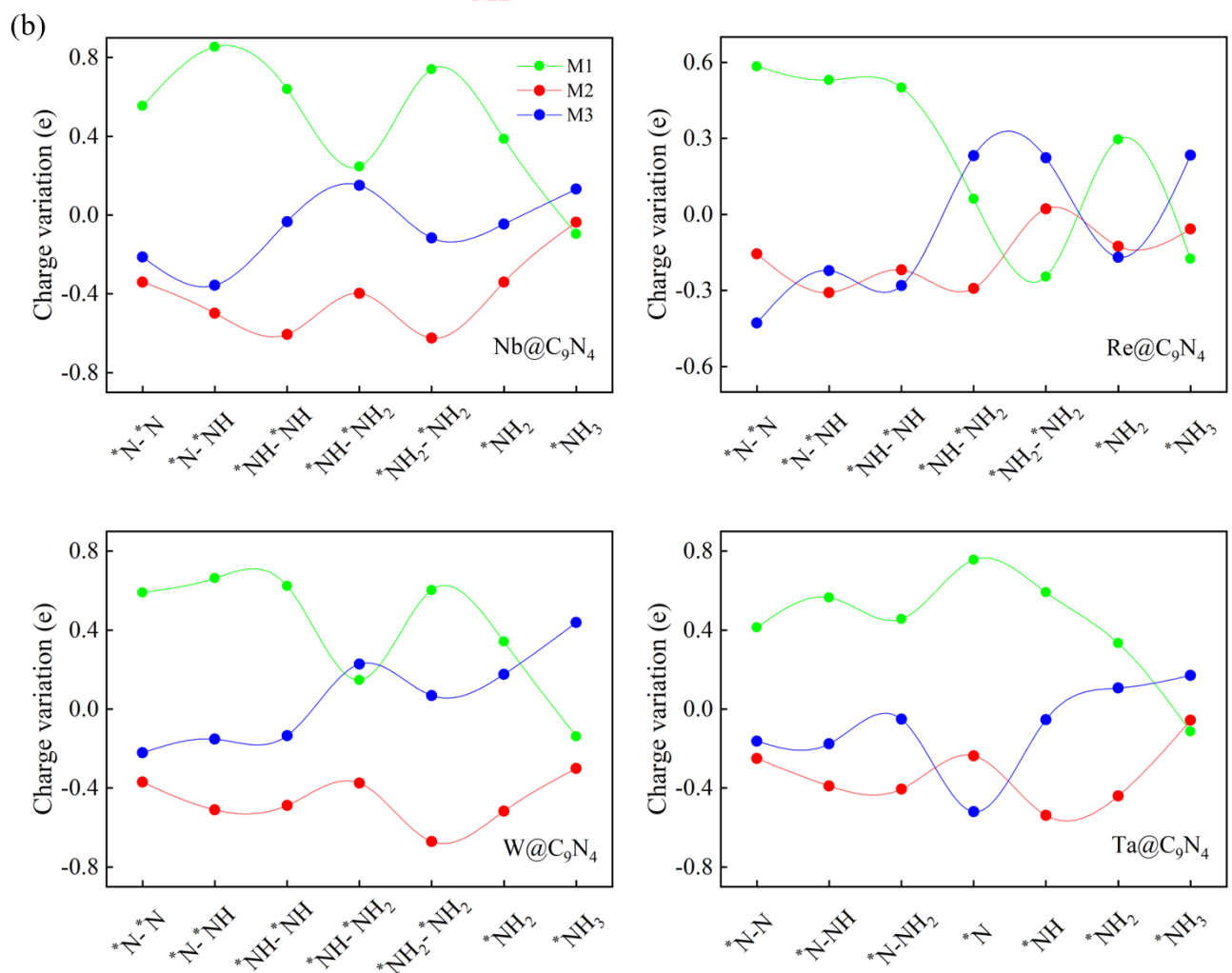
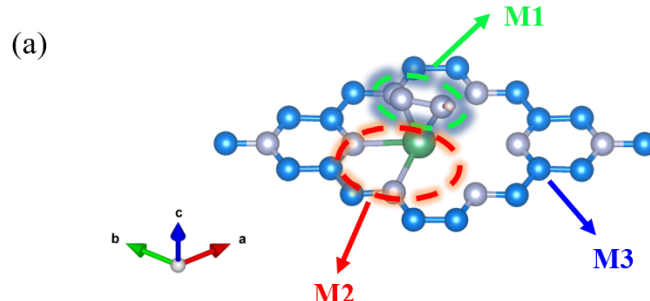


**Fig. S5** (a) Defined three moieties in  $\text{N}_x\text{H}_y$  species adsorbed on TM@g-C<sub>9</sub>N<sub>4</sub>. (b) Charge variation of three moieties over Nb, Re, W@g-C<sub>9</sub>N<sub>4</sub> via the enzymatic pathway and Ta@g-C<sub>9</sub>N<sub>4</sub> via the distal pathway.

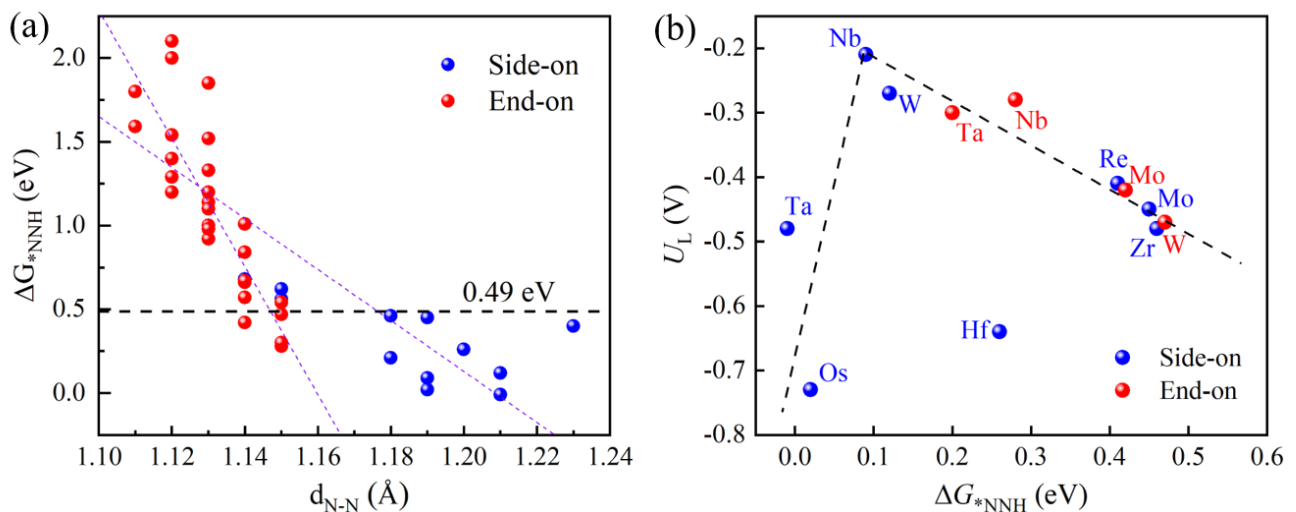


**Fig. S6** (a) The free energy of  $*\text{NNH}$  species ( $\Delta G_{*\text{NNH}}$ ) as a function of N–N bond length ( $d_{\text{N–N}}$ ). (b) The computed NRR limiting potential ( $U_L$ ) as a function of the adsorption free energy of  $*\text{NNH}$  species ( $\Delta G_{*\text{NNH}}$ ), blue and red balls represent side-on and end-on configurations, respectively.